J Physiol 590.17 (2012) pp 4307–4319

The Journal of Physiology

A distinct *de novo* expression of $Na_v1.5$ sodium channels in human atrial fibroblasts differentiated into myofibroblasts

Aurélien Chatelier[1], Aurélie Mercier[1], Boris Tremblier[1], Olivier Thériault[2], Majed Moubarak[1], Najate Benamer[1], Pierre Corbi[3], Patrick Bois[1], Mohamed Chahine[2] and Jean François Faivre[1]

[1]*Institut de Physiologie et Biologie Cellulaires, FRE 3511, CNRS/Université de Poitiers, Poitiers, France*
[2]*Institut universitaire en santé mentale de Québec, Université Laval, Québec, Canada*
[3]*Service de chirurgie cardio-thoracique, CHU Poitiers, France*

Key point

- Fibroblasts play a major role in heart physiology. In pathological conditions, they can lead to cardiac fibrosis when they differentiate into myofibroblasts.
- This differentiated status is associated with changes in expression profile leading to neo-expression of proteins such as ionic channels.
- The present study investigates electrophysiological changes associated with fibroblast differentiation focusing on voltage-gated sodium channels in human atrial fibroblasts and myofibroblasts.
- We show that human atrial fibroblast differentiation in myofibroblasts is associated with *de novo* expression of voltage gated sodium current. Multiple arguments support that this current is predominantly supported by the $Na_v1.5$ α-subunit which may generate a persistent sodium entry into myofibroblasts.
- Our data revealed that $Na_v1.5$ α-subunit expression is not restricted to cardiac myocytes within the atrium. Since fibrosis is one of the fundamental mechanisms implicated in atrial fibrillation, it is of great interest to investigate how this channel could influence myofibroblasts function.

Abstract Fibroblasts play a major role in heart physiology. They are at the origin of the extracellular matrix renewal and production of various paracrine and autocrine factors. In pathological conditions, fibroblasts proliferate, migrate and differentiate into myofibroblasts leading to cardiac fibrosis. This differentiated status is associated with changes in expression profile leading to neo-expression of proteins such as ionic channels. The present study investigates further electrophysiological changes associated with fibroblast differentiation focusing on the activity of voltage-gated sodium channels in human atrial fibroblasts and myofibroblasts. Using the patch clamp technique we show that human atrial myofibroblasts display a fast inward voltage gated sodium current with a density of 13.28 ± 2.88 pA pF^{-1} whereas no current was detectable in non-differentiated fibroblasts. Quantitative RT-PCR reveals a large amount of transcripts encoding the $Na_v1.5$ α-subunit with a fourfold increased expression level in myofibroblasts when compared to fibroblasts. Accordingly, half of the current was blocked by 1 μM of tetrodotoxin and immunocytochemistry experiments reveal the presence of $Na_v1.5$ proteins. Overall, this current exhibits similar biophysical characteristics to sodium currents found in cardiac myocytes except for the window current that is enlarged for potentials between -100 and -20 mV. Since fibrosis is one of the fundamental mechanisms implicated in atrial fibrillation, it is of great interest to investigate how this current could influence myofibroblast properties. Moreover, since

DOI: 10.1113/jphysiol.2012.233593

several $Na_v1.5$ mutations are related to cardiac pathologies, this study offers a new avenue on the fibroblasts involvement of these mutations.

(Received 2 April 2012; accepted after revision 10 July 2012; first published online 16 July 2012)

Corresponding author A. Chatelier: FRE CNRS/Université de Poitiers no. 3511, Pôle Biologie Santé, Bâtiment B36, 1 rue Georges Bonnet, BP 633, 86022 Poitiers Cedex. Email: aurelien.chatelier@univ-poitiers.fr

Abbreviations BDM, 2,3-butanedione 2-monoxime; *k*, Boltzmann steepness coefficient; qPCR, quantitative PCR; RT-qPCR, reverse transcriptase-quantitative polymerase chain reaction; α-SMA, α-smooth muscle actin; TTX, tetrodotoxin; $V_{1/2}$, membrane potential at half-maximal activation or inactivation; VGSC, voltage gated sodium channel.

Introduction

Fibroblasts represent the most abundant cell type founded in cardiac tissue. Although these cells have received less attention than cardiomyocytes, they are important players in many processes such as control of extracellular matrix renewal and production of various paracrine and autocrine factors (Brilla *et al.* 1995; Ellmers *et al.* 2002; Baudino *et al.* 2006). Within the heart, at least two fibroblast populations can be distinguished depending on their tissue localization in the atria or the ventricles. Atrial and ventricular fibroblasts display fundamental differences in their morphology, gene expression profiles and proliferation properties (Burstein *et al.* 2008). It was hypothesized that these characteristics explain, at least in part, the greater propensity of atria to fibrosis compared to the ventricles (Nakajima *et al.* 2000; Verheule *et al.* 2004; Xiao *et al.* 2004). This susceptibility is important since fibrosis and tissue remodelling is one of the fundamental mechanisms implicated in atrial fibrillation (Allessie *et al.* 2002; Burstein & Nattel, 2008), the most common sustained arrhythmia in human (for review see Schotten *et al.* 2011).

In pathological situations such as heart failure, both atrial and ventricular fibroblasts proliferate, migrate and differentiate into myofibroblasts that synthesize excessive extracellular matrix proteins leading to cardiac fibrosis (Weber *et al.* 1994; Swynghedauw, 1999; Manabe *et al.* 2002). This differentiation into myofibroblasts is accompanied by changes in gene expression pattern leading notably to neo-expression of proteins such as α-smooth muscle actin (α-SMA) (Baudino *et al.* 2006). Whereas fibroblasts and myofibroblasts have long been considered as non-excitable cells, studies focused on their electrophysiological properties have emerged in the past decade (for reviews see Yue *et al.* 2011; Vasquez *et al.* 2011). Ventricular fibroblasts express several potassium channels (Chilton *et al.* 2005; Shibukawa *et al.* 2005; Benamer *et al.* 2009; Li *et al.* 2009*a*) and non-selective cationic channels (Rose *et al.* 2007). Voltage gated sodium channels (VGSCs) and chloride channels have also been recently reported in commercially available cultured ventricular fibroblasts (Li *et al.* 2009*a*). Beside the well-characterized role of these channels in excitable cells, there is increasing evidence that VGSCs are also expressed and contribute to cellular functions in non-excitable cells. For example, they appear to be important modulators of cancer cell invasion processes (Roger *et al.* 2003; Gillet *et al.* 2009), human endothelial cells angiogenic abilities (Andrikopoulos *et al.* 2011) or microglia and epidermal keratinocytes secretion properties (Zhao *et al.* 2008; Black *et al.* 2009). VGSCs are composed of one α-subunit, which forms the core of the channel, and several β-subunits, which modulate their expression levels and gating properties (Catterall, 1986; Fozzard & Hanck, 1996; Armstrong & Hille, 1998). In their study on ventricular fibroblasts, Li *et al.* (2009*a*) found that five different VGSC α subunits were heterogeneously expressed within the cultured cells.

Atrial fibroblasts have been less studied than ventricular fibroblasts. Electrophysiological studies report that they express a stretch activated non-selective cationic current (Kamkin *et al.* 2003*a*), a voltage-dependent proton current (El Chemaly *et al.* 2006) and the non-selective cationic channel TRPM7 (Du *et al.* 2010).

Since fibroblasts and myofibroblasts are involved in several physiological and physiopathological processes, it is important to distinguish ionic channel expression within their differentiated state. For example, we have shown that potassium channels, and notably SUR2/Kir6.1, appear progressively over ventricular fibroblast differentiation into myofibroblast and modulate cell proliferation and secretion properties (Benamer *et al.* 2009). Similarly, in atria, it was shown that TRPM7 plays an essential role in human atrial fibroblast proliferation and differentiation (Du *et al.* 2010).

Based on the observations that fibrosis depends on differentiation of fibroblasts into myofibroblasts (Vasquez *et al.* 2011) and is more likely to occur within atria (Yue *et al.* 2011), the present study aimed at investigating electrophysiological changes associated with human atrial fibroblast differentiation. We focused our study on the activity of VGSCs in human atrial fibroblasts or myofibroblast primary cultures. Using reverse transcriptase-quantitative polymerase chain reaction (RT-qPCR), Western blot, immunocytochemistry and the patch clamp technique, we characterized the molecular identity and electrophysiological properties of VGSCs in these cells. The physiological and physiopathological impact of VGSCs in cardiac fibroblasts will be discussed.

Table 1. Characteristics of patients.

Patient	Pathology	Age	Sex	Time of culture tested (days)
1	AAA	56	F	12<
2	AVS	79	F	12<
3	CAS	69	F	12<
4	MVE + CAS	83	F	12<
5	AVS	73	M	12<
6	CAS	56	F	12<
7	AI	60	M	<7 and 12<
8	AAA	59	M	<7 and 12<
9	CAS	66	M	<7 and 12<
10	AVS	74	M	<7 and 12<
11	CAS	64	M	7< and >12
12	CAS	64	M	7< and >12
13	CAS	72	M	<7
14	CAS	70	F	<7
15	CAS	72	F	<7
16	AVS	70	M	<7

AAA, ascending aortic aneurysm; AI, aortic insufficiency; AVS, aortic valve stenosis; CAS, coronary artery stenosis; MVE, mitral valve endocarditis; F, female; M, male. 12<, cells were used after 12 days of culture. <7 and 12<, cells were used before 7 days or after 12 days of culture. 7< and >12, cells were used between 7 and 12 days of cultutre. <7, cells were used before 7 days of culture.

Methods

Ethical approval

All procedures were approved by the human research committee, 'comité de protection des personnes Ouest III', at the University of Poitiers and were carried out in accordance with the *Declaration of Helsinki*. Informed consent was obtained from each patient.

Patients

Right atrial human appendages were obtained from 16 patients (67.9 ± 1.9 years old, 9 males and 7 females) undergoing a cardiac bypass surgery. Sinus rhythm was present in all cases. Myocardial samples were removed during cannulation for cardiopulmonary bypass with extra-corporal circulation, a routine procedure comprising normal management of the patients. Characteristics of patients are given in Table 1.

Isolation and culture of human atrial fibroblasts

Cardiac cells, consisting of smooth muscle cells, endothelial cells, fibroblasts and cardiomyocytes, were dissociated as previously described (Hatem *et al.* 1997; Ancey *et al.* 2002; El Chemaly *et al.* 2006). Heart tissue was minced in calcium-free Krebs solution containing (mmol l^{-1}): NaCl 35, KCl 7.75, KH_2PO_4 1.18, Na_2HPO_4 20, Hepes 10, glucose 10, $NaHCO_3$ 25, saccharose 70, 2,3-butanedione 2-monoxime (BDM) 30, and EGTA 0.5 (pH was adjusted to 7.4 with NaOH), and enzymatically dissociated afterwards over several digestion steps. The first one was performed for 25 min with tissues maintained in the same solution without BDM or EGTA and supplemented with 0.5% bovine serum albumin (BSA), 200 IU ml^{-1} collagenase (type V, Sigma-Aldrich Co., Saint-Quentin Fallavier, France), and 6 IU ml^{-1} protease (type XXIV, Sigma-Aldrich). Two other 20 min digestion steps followed using the same enzymatic solution but containing only collagenase (400 IU ml^{-1}). All steps were carried out with solutions gently shaken in a water bath maintained at 37°C in a 95% O_2 and 5% CO_2 atmosphere. This was followed by gentle stirring of the tissue in a washing buffer containing (mmol l^{-1}): NaCl 130, KCl 4.8, KH_2PO_4 1.2, Hepes 25, glucose 5, EGTA 0.15 and BSA 2% (pH was adjusted to 7.4 with NaOH). Dissociated cells were submitted to successive filtration and centrifugation steps to eliminate cell debris, cardiomyocytes, endothelial and smooth muscle cells as described in previous studies (Louault *et al.* 2008; Benamer *et al.* 2009). Human atrial fibroblasts were cultured afterwards in Dulbecco's Modified Eagle's medium (DMEM; Biowhittaker, Emerainville, France) supplemented with 10% fetal bovine serum (Biowest, Nuaillé, France), 1% antibiotics (100 IU mol^{-1} penicillin-G-Na; 50 IU ml^{-1} streptomycin sulfate), and 1% insulin (10^{-7} mol l^{-1}). The culture was incubated at 37°C in a humidified, 5% CO_2-enriched atmosphere. The culture medium was replaced every 48 h. For patch clamp experiments, just after cell dissociation fibroblasts were seeded directly in 35 mm dishes (NunclonΔ polystyrene surface) kept in culture without trypsin steps until patch clamp experiments. For Western blots and RT-qPCR just after cell dissociation fibroblasts were seeded in 92 mm dishes (NunclonΔ polystyrene surface) and kept in culture without trypsin steps until Western blot or RT-qPCR experiments.

Western blots

Fibroblasts in primary culture were washed with cold phosphate-buffered saline (PBS) and lysed by scraping the cells into a lysis buffer (in mmol l^{-1}: Tris-HCl 50, NaCl 150, EDTA 5, 0.05% Igepal, 1% deoxycholic acid, 1% Triton X-100, 0.1% SDS) containing protease inhibitors (Protease Inhibitor Cocktail, Sigma-Aldrich). Cell lysates were then incubated for 30 min on ice and centrifuged at 1750 *g* for 10 min at 4°C. Soluble cell lysates were denatured 30 min at 37°C in 2× sample buffer (in mmol l^{-1}): Tris-HCl 126, SDS 4%, glycerol

20%, bromophenol blue 0.02%, β-mercaptoethanol 5%. Protein samples (10 μg), obtained from fibroblasts in primary culture, were separated by SDS-PAGE using 8% polyacrylamide gels and transferred to nitrocellulose membranes. Membranes were blocked 1 h in TBS-Tween blocking solution (in mmol l^{-1}: Tris-HCl 100, NaCl 150 and Tween-20 0.1%) with 5% non-fat milk and then probed overnight at 4°C with primary antibodies. Because of the small amount of tissue and so the limited number of atrial fibroblasts obtained after dissociation, the use of the specific anti-human $Na_v1.5$ antibody was not possible in our conditions for Western blot experiments. Therefore, we used the powerful primary antibodies rabbit polyclonal anti-SP19 (1:1000, Alomone Labs Ltd, Jerusalem, Israel) that recognizes all VGSC subunits. β-Actin was probed by mouse monoclonal anti-β-actin (1:10000, Sigma). Membranes were washed and incubated for 1 h at room temperature with specific anti-rabbit or anti-mouse horseradish peroxidase-conjugated secondary antibodies (1:5000, Interchim, Montluçon, France). Membranes were revealed with enhanced chemiluminescence (ECL) chemiluminescent substrate (GE Healthcare, Velizy-Villacoublay, France).

Immunofluorescence staining

Fibroblasts were cultured on coverslips and grown in DMEM. The cells were fixed with PBS with 3% paraformaldehyde for 10 min, permeabilized by 20 min incubation in PBS containing 0.1% Triton X-100, and blocked in PBS containing 5% BSA. Samples were then incubated overnight at 4°C with primary antibodies in PBS containing 5% BSA, after which they were incubated for 1 h at room temperature with the appropriate secondary antibody in the same solution. Coverslips were rinsed and mounted using fluorescence mounting medium (Vectashield, Vector Laboratories, Inc., Burlingame, CA, USA) on glass microscope slides and examined by confocal microscopy.

Primary antibodies used were anti-fibronectin rabbit polyclonal antibody 1/100 (Santa Cruz Biotechnology, Inc., Santa Cruz, CA, USA) to identify fibroblasts, anti-α-SMA monoclonal mouse antibody (Dako, Trappes, France) 1/100 to characterize myofibroblasts and anti-human $Na_v1.5$ rabbit antibody (Alomone) 1/200 to label $Na_v1.5$ sodium channels. Secondary antibody used were Alexa fluor 488 chicken anti-rabbit IgG (1/1000), Alexa Fluor 555 donkey anti-mouse (1/200) and Alexa fluor donkey 568 anti-rabbit IgG (1/400) from Molecular Probes (Invitrogen, Saint Aubin, France). The specificity of secondary antibodies was confirmed by the absence of a signal in preparations when the primary antibody was omitted. Nuclear staining was obtained using TO-PRO-3 (Invitrogen).

Patch clamp experiments

The measurements were carried out at room temperature (~22°C). Fire-polished, patch electrodes (~2 MΩ) were pulled from borosilicate glass capillaries using a vertical micropipette puller (Narishige, Tokyo, Japan). The pipettes were coated with the silicone elastomer HIPEC R6101 (Dow-Corning, Midland, MI, USA) to minimize capacitance. Voltage clamp experiments were performed using an Axopatch 200B amplifier with a CV 203BU headstage (Molecular Devices, Sunnyvale, CA, USA). Series resistance compensation was performed to values >80% to minimize voltage errors. Voltage command pulses were generated by a personal computer equipped with an analog–digital converter (Digidata 1200, Molecular Devices) using pCLAMP software v8.0 (Molecular Devices). Linear leak currents and capacitance artefacts were removed using *P*/*N* leak subtraction. Sodium currents were filtered at 5 kHz and digitized at 20 kHz. Cell capacitance was recorded as a telegraph readout of cell capacitance compensation using Axopatch 200B and pCLAMP. The digitized currents were stored on a computer for later off-line analysis. To avoid clamp problems, only recordings that exhibit an access resistance lower than 5 MΩ were kept for biophysical parameters analysis. The patch pipettes were filled with (mM): 35 NaCl, 105 CsF, 0.1 EGTA, and 10 Hepes. The pH was adjusted to 7.4 using CsOH. The bath solution contained (mM): 150 NaCl, 2 KCl, 1.5 $CaCl_2$, 1 $MgCl_2$, 10 glucose, and 10 Hepes. The pH was adjusted to 7.4 using NaOH. In these conditions, theoretical reversal potential was expected to be around 37 mV. However, the particular myofibroblast shape, which is extremely flat, probably restricted the sodium diffusion from the pipette solution to the intracellular compartment leading to a more positive reversal potential. A −7 mV correction of the liquid junction potential between the patch pipette and the bath solutions was performed.

Currents were recorded using the whole-cell configuration of the patch clamp technique. Sodium currents were generated by clamping cell membrane from a holding potential of −120 mV to potentials ranging from −100 mV to 40 mV for 50 ms in 10 mV increments with 3 s stimulus intervals. Fast and slow decay time constants were obtained by fitting current traces with a double exponential equation. The voltage dependence of activation was determined from the relative membrane conductance as a function of potential using the formula $G_{Na} = I_{Na}/(V_m - V_{rev})$, where G_{Na} is peak conductance and I_{Na} is peak sodium current for the test potential V_m. V_{rev} is the estimated reversal potential of the sodium current obtained by the extrapolation of the current–voltage relationship. The resulting sodium ion conductance was normalized to the maximum response for each

cell. The activation data were fitted with a Boltzmann equation: $G/G_{max} = 1/(1 + \exp[(V - V_{1/2})/k])$, where G_{max} represents the maximum conductance and $V_{1/2}$ and k represent the half-maximum voltage of activation and the Boltzmann steepness coefficient, respectively.

The voltage dependence of inactivation was obtained by measuring the peak Na^+ current during a 20 ms test pulse to −20 mV, which followed a 500 ms pre-pulse to membrane potentials between −120 and 0 mV from a holding potential of −120 mV. Peak inward currents, I, were measured and normalized to the maximum response, I_{max}, of each cell. The inactivation data were also fitted with a Boltzmann equation.

Real-time reverse transcription polymerase chain reaction (RT-qPCR)

Total RNA from human cardiac fibroblasts was isolated using RNAble reagent (Eurobio, Courtaboeuf, France) followed by chloroform extraction and isopropanol precipitation. RNA integrity was evaluated by ethydium bromide staining on a 1% agarose gel. Total RNA was quantified by assessing optical density at 260 and 280 nm (NanoDrop ND-100, Labtech France, Palaiseau, France). cDNA was synthesized using the $Pd(N)_6$ random hexamer primer (GE Healthcare Life Sciences). Ten microlitres of total RNA (1–2 μg) was added to 12 μl of reaction mixture (100 mmol l^{-1} Tris-HCl pH 8.3, 150 mmol l^{-1} KCl, 6.25 mmol l^{-1} $MgCl_2$, 20 mmol l^{-1} DTT, 2 mmol l^{-1} dNTPs (Invitrogen) and 2.4 μg Random Primer $p(dN)_6$ (GE Healthcare Life Sciences). RNA were denatured at 65°C during 2 min and then added to 40 U RNAse inhibitor (RNaseOUT, Invitrogen) and 400 U M-MLV reverse transcriptase (Invitrogen) to 25 μl final volume. cDNA was synthesized at 37°C for 1 h and then added with 50 μl sterile water. Remaining enzymes were heat-deactivated (100°C, 2 min).

qPCR assays were carried out using SYBR green I detection dye on a LC480 platform (Roche) using the vendor's specifications. Primers were designed using PerlPrimer v1.1.19. All qPCR samples were run at least in duplicate, and for each plate we applied a non-template control (NTC) and positive control for each primer pair to control every qPCR run.

Analysis has been done with the lightcycler software LightCycler® 480 SW 1.5 using the second derivative method. Run-to-run variation has been adjusted using a known standard and quantification was corrected for efficiency calculated with the standard curves. Human heart APEX ($Na_v1.4$, $Na_v1.5$, GAPDH) and human cortex ($Na_v1.1$, $Na_v1.2$, $Na_v1.3$, $Na_v1.7$, $Na_v1.8$, $Na_v1.9$, Nax) mRNA has been used for RT-PCR. cDNA was amplified by PCR using specific primer and DNA dilution was used for standard curves. The specificity of the amplification for each run was controlled with a melting curve analysis and was performed directly following the PCR by continuously reading the fluorescence while slowly heating the reaction from 65°C to 95°C.

HEK293T cell transfection

HEK293T cells were grown in high glucose DMEM supplemented with fetal bovine serum (10%), L-glutamine (2 mM), penicillin (100 U ml^{-1}) and streptomycin (10 mg ml^{-1}). The cells were incubated in a 5% CO_2 humidified atmosphere after being transfected with wild-type human $Na_v1.5$ cDNA (1.5 μg) and human $\beta1$ subunit (1.5 μg) using the calcium phosphate method as previously described (Margolskee *et al.* 1993). The human sodium channel $\beta1$ subunit and CD8 were inserted in the pIRES bicistronic vector in the form of pCD8-IRES-$\beta1$. Using this strategy, transfected cells that bound beads also expressed the $\beta1$ subunit protein. Before performing patch-clamp experiments, 2 day post-transfection cells were incubated for 5 min in medium containing anti-CD8 coated beads (Dynabeads CD8, Invitrogen, Dynal AS, Oslo, Norway). The unattached beads were removed by washing with extracellular solution. Cells expressing CD8 were distinguished from non-transfected cells by visualizing beads fixed on the cell membrane by light microscopy. Using this strategy, transfected cells that bound beads also expressed the $\beta1$ subunit protein.

Data analysis

Data were analysed using a combination of pCLAMP software v8.0 (Molecular Devices), Microsoft Excel and SigmaPlot 8.0 (SPS, Chicago, IL, USA).

Data are presented as means ± standard error of the mean (SEM). Differences between mean values were evaluated by Student's t test or one-way analysis of variance (ANOVA) with values of $P < 0.05$ indicating a significant difference.

Results

Appearance of a voltage gated sodium current in human atrial fibroblast cultures

Human atrial fibroblast differentiation into myofibroblast in culture was evaluated through expression of α-SMA observed by immunofluorescence labelling (Fig. 1*A*). Experiments carried out after 7 days of culture show a clear staining of fibronectin, a specific marker of fibroblastic cells. At this time of culture no specific labelling of α-SMA, a specific marker of myofibroblasts, was observed whereas this protein is strongly expressed after 12 days. This indicates that the differentiation of human atrial fibroblasts into myofibroblasts occurs between 7 and 12 days of culture in our conditions. To investigate the presence of VGSCs during fibroblast differentiation, western

blot experiments were performed after 5 or 15 days of culture (Fig. 1*B*). At 5 days of culture the VGSC protein was absent whereas it was expressed in myofibroblasts of 15 days of culture. To test whether this expression was correlated to the presence of a fast inward sodium current during fibroblast differentiation, whole-cell patch clamp experiments were performed after different times of culture. Before 8 days, no cell ($n = 7$ cells/4 patients) presented a fast inward sodium current whereas 75% of cells ($n = 12$ cells/2 patients) showed this current between 8 and 12 days of culture (Fig. 1*C*). This proportion reached 100% of cells ($n = 22$ cells/7 patients) after 12 days. No relation between the VGSC current appearance and the pathology or the sex of the patients was observed.

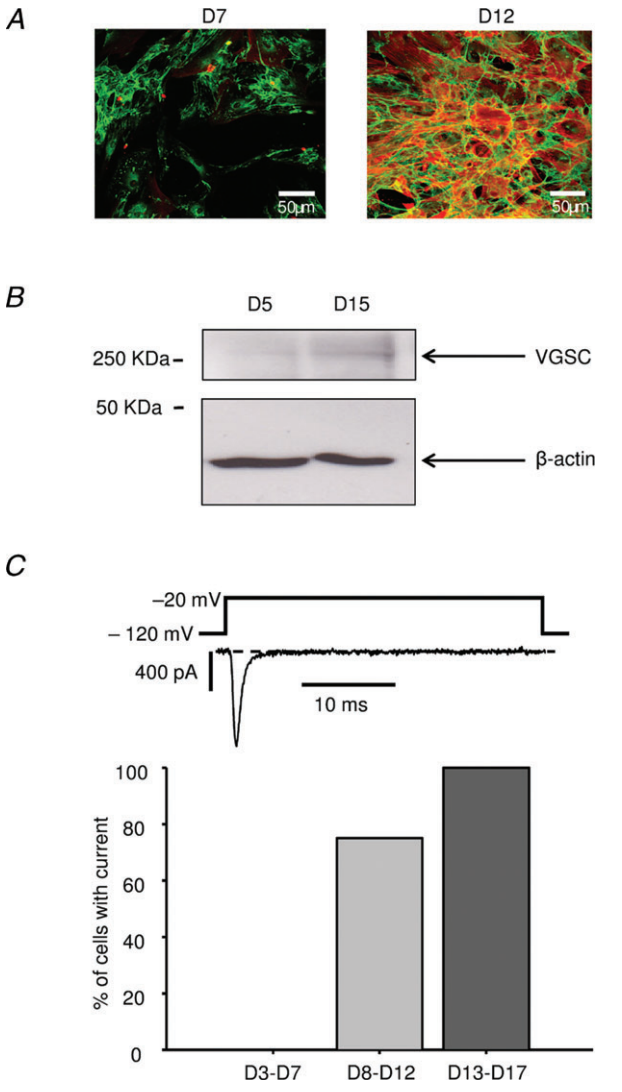

Figure 1. Appearance of a fast inward voltage gated sodium current with human atrial fibroblast differentiation
A, cells were stained after 7 (left panel) or 12 (right panel) days of culture with anti-fibronectin (green labelling) and anti-α-SMA (red labelling) antibodies. *B*, Western blot, representative of 3 experiments, performed with protein preparations obtained from human atrial fibroblasts at 5 and 15 days of culture using antibodies to VGSC and β-actin. *C*, percentage of cells that exhibit a voltage gated transient inward current after 3–7 days (D3–D7, $n = 7$), 8–12 days (D8–D12, $n = 12$) or 13–17 days (D13–D17, $n = 22$) of culture. An example of current after 15 days of culture is shown (top panel).

Biophysical properties of human atrial myofibroblasts VGSC current

Whole cell patch-clamp recordings of the human atrial myofibroblasts using voltage steps from a holding potential of −120 mV produced typical fast activation and fast inactivating currents (Fig. 2*A*). Whereas no current was observed at −20 mV after 5 days of culture (0.05 ± 0.18 pA pF^{-1}, $n = 5$), current density increased to 4.60 ± 1.19 pA pF^{-1} ($n = 3$) after 10 days and reached 13.28 ± 2.88 pA pF^{-1} ($n = 8$) after 15 days ($P < 0.01$, one-way ANOVA). However, sodium currents recorded

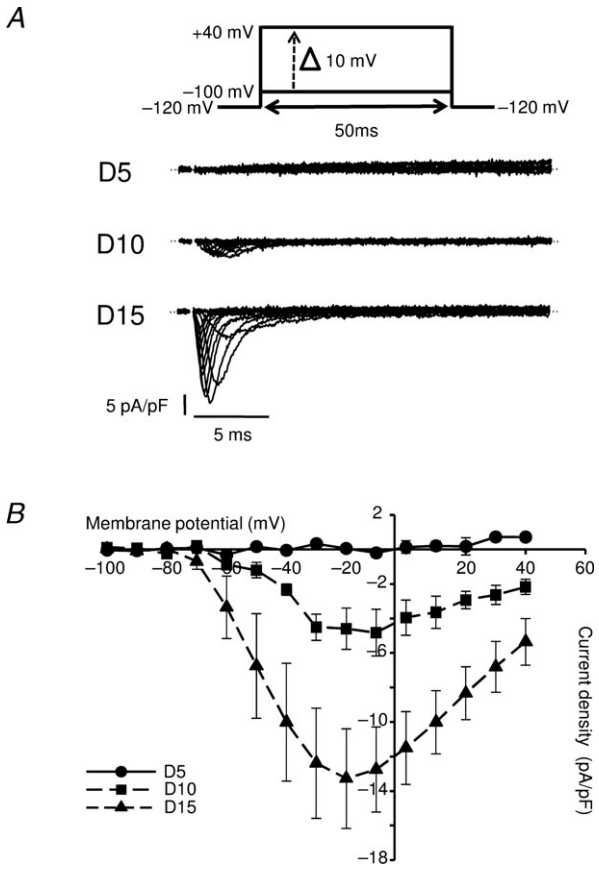

Figure 2. Whole-cell properties of VGSCs recorded in human atrial fibroblasts
A, representative traces of whole cell currents recorded after 5 (D5), 10 (D10) or 15 (D15) days of fibroblast culture using the protocol shown on top. *B*, current density–voltage relationship recorded after 5 (circles, $n = 5$), 10 (squares, $n = 3$) and 15 (triangles, $n = 8$) days of culture. Currents were elicited as described in *A*.

after 10 ($n = 3$) and 15 ($n = 8$) days of culture display current–voltage curves with similar voltage sensitivity (Fig. 2*A* and *B*). Sodium current activation occurs for potentials positive to −70 mV and the peak current was observed at a potential closed to −20 mV. The reversal potential estimated at D15 by extrapolation of the linear part of current–voltage relationship was 71.0 ± 6.4 mV ($n = 8$). The voltage dependence of activation recorded at D15 was determined as described in Methods (Fig. 3*A*). The activation begins at −70 mV and is maximal for potentials greater than 0 mV. When the data are fitted with a Boltzmann function, the midpoint for activation ($V_{1/2}$) and the Boltzmann steepness coefficient (k) are respectively −41.7 ± 4.0 mV and 7.6 ± 0.8 mV ($n = 8$). The availability was determined at D15 from the normalized peak current amplitude of standard test pulses at −20 mV and plotted *versus* prepulse voltages (Fig. 3*A*). The smooth curve fits a Boltzmann function as described in Methods with a midpoint ($V_{1/2}$) and a Boltzmann steepness coefficient (k) of −83.9 ± 3.1 mV and −7.8 ± 0.7 mV, respectively ($n = 5$).

The overlap of the activation and inactivation curves identifies a voltage range where a proportion of sodium channels can enter into an activated state without being fully inactivated ('window current'; Fig. 3*B*). The steady-state availability of channels within this window of voltages is calculated as the product of the fitted steady-state activation and inactivation parameters as described previously (Huang *et al.* 2010). This availability is a biphasic function and is very small for potentials below −100 mV and above −20 mV. Between these potentials, there is a non-negligible probability to have persistent opened channels with a peak value of 0.37% obtained at −60 mV.

The time courses of current decay elicited at depolarized voltages were fitted using a double exponential function. The resulting fast and slow time constants were plotted *versus* voltage (Fig. 3*C*) and were 2.8 ± 0.5 ms and 13.9 ± 3.3 ms at −40 mV, respectively ($n = 8$).

$Na_v1.5$ and β_1 subunits are good candidates for the myofibroblast VGSC current

In order to identify VGSC α and β subunit transcripts expressed in fibroblasts and myofibroblasts, RT-qPCR was carried out on cells from three different patients obtained before 8 and after 13 days of culture, respectively. Figure 4*A* illustrates the expression pattern of nine of the sodium channel α subunits. Interestingly, amongst these screened transcripts, only $Na_v1.2$ and $Na_v1.5$ were detected in fibroblasts with an expression level of $Na_v1.5$ sevenfolds higher than $Na_v1.2$. In myofibroblasts, other isoforms were detected such as $Na_v1.3$, 1.6 and 1.7 whereas $Na_v1.2$ expression was unchanged. On the other hand, $Na_v1.5$ presented a fourfold increased expression level and was at least eightfold higher than other α subunit transcripts. Subunits like $Na_v1.1$, 1.4, 1.8, 1.9 or the atypical Na_x were not detected in fibroblasts or myofibroblasts.

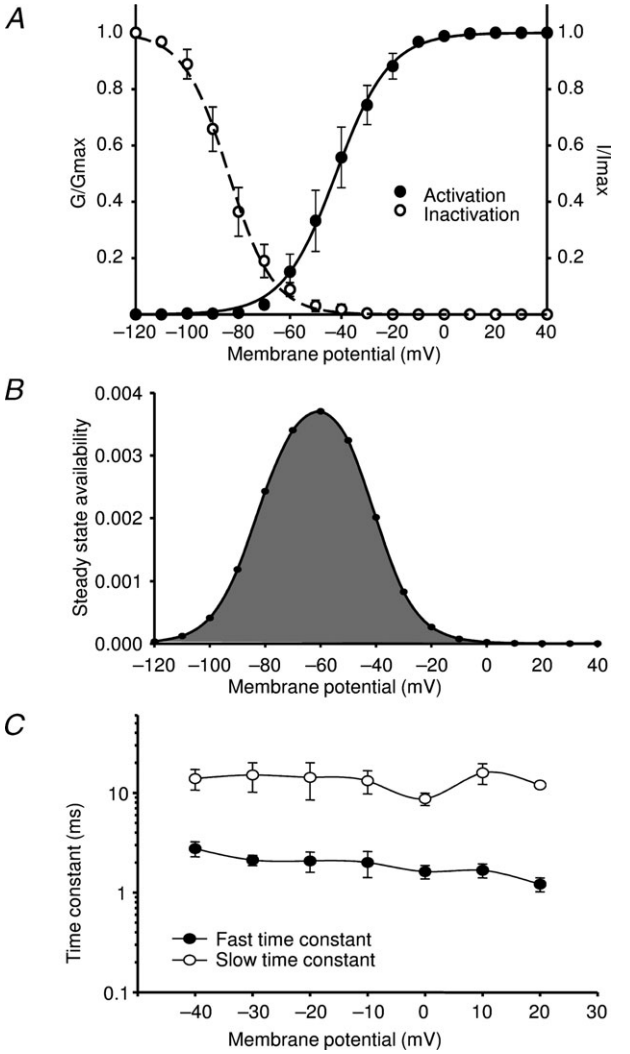

Figure 3. Biophysical properties of VGSCs recorded in human atrial myofibroblasts after 15 days in culture
A, voltage dependence of activation (filled circles, $n = 8$) and inactivation (open circles, $n = 5$) fitted with a Boltzmann function (see Methods). Sodium conductance (G) was calculated from the *I–V* curve experiments (Figure 2A). This conductance was normalized to maximum conductance (G_{max}) obtained during the *I–V* curve and plotted *versus* imposed membrane potential. Steady state inactivation was assayed as described in Methods and plotted *versus* membrane pre-pulse potential. *B*, the overlap of activation and inactivation of sodium channels defines a range of voltages (window) where the channels could be partially activated without being fully inactivated. The availability of channels at a stable potential is calculated as the product of the activation and the inactivation Boltzmann functions (Huang *et al.* 2010). *C*, fast (filled circles) and slow (open circles) inactivation time constants as a function of membrane potential. The decay phases of currents elicited as described in Fig. 2*A* ($n = 8$) were fitted with a double exponential to estimate the open state inactivation time constants.

β subunit transcripts are also expressed in fibroblasts and myofibroblasts (Fig. 4*B*). The major β subunit was β_1 with quantities that doubled with fibroblast differentiation. Small amounts of β_3 and β_4 were also present whereas β_2 was absent.

Human atrial myofibroblast VGSC current is predominantly supported by the $Na_v1.5$ α subunit

Based on the RT-qPCR results (Fig. 4*A*), $Na_v1.5$ is the more abundant transcript in myofibroblasts. Because this is the only detected transcript which codes for a TTX resistant α-subunit, the cells were perfused with 1 μM TTX to investigate whether the current recorded in myofibroblasts was sensitive to TTX. Figure 5*A* and *B* shows that the perfusion of 1 μM of TTX produced a significant and reversible reduction of the sodium current to $41.8 \pm 8.0\%$ of the control amplitude ($n = 4$, $P < 0.01$, one-way ANOVA). To compare the reduction of current observed to the $Na_v1.5$ TTX sensitivity, we used HEK293T cells transiently transfected with both human α-$Na_v1.5$ and β_1 subunits. In our conditions, 1 μM TTX decreased $Na_v1.5$ current to $47.98 \pm 9.83\%$ of the control ($n = 3$, $P < 0.01$, one-way ANOVA), which is not significantly different from the reduction observed in myofibroblasts. The $Na_v1.5$ α subunit expression in myofibroblasts was finally investigated by immunofluorescence experiments (Fig. 5*C*). Cells incubated with specific $Na_v1.5$ antibodies after 15 days of culture exhibited a clear staining that confirmed the presence of the protein whereas it was absent at 5 days of culture.

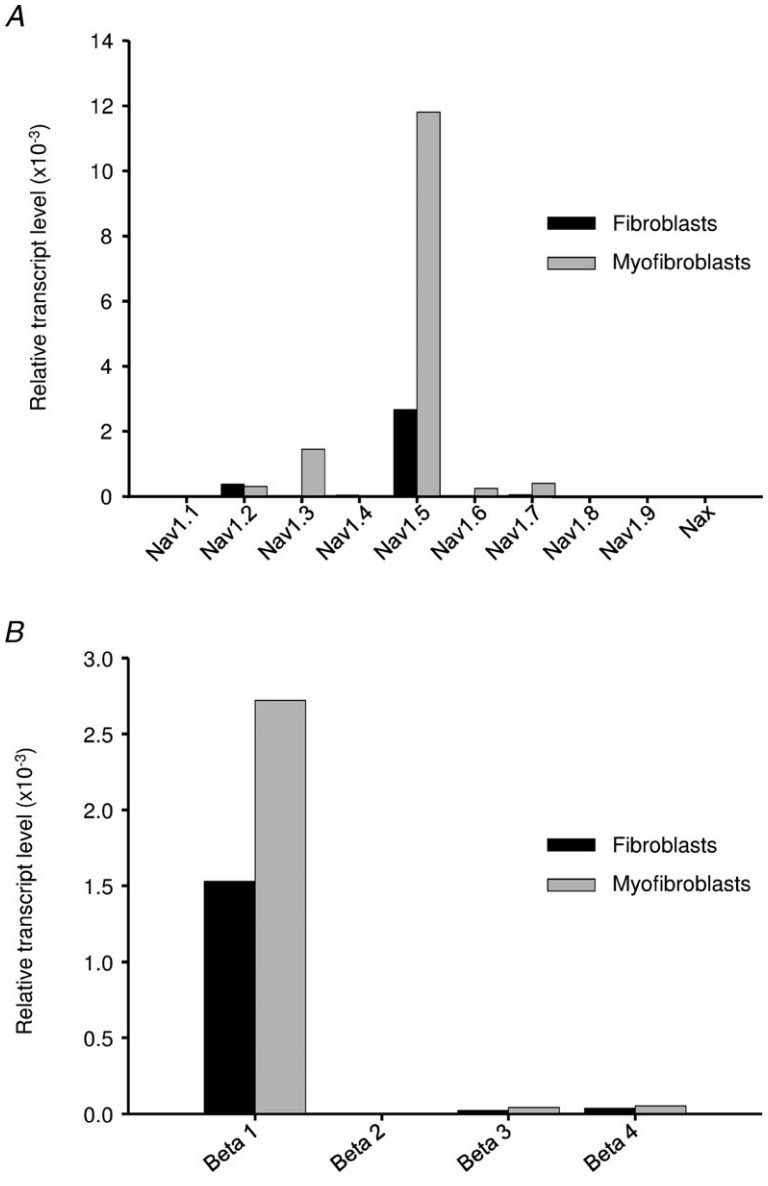

Figure 4. mRNA expression levels of VGSC subunits in human atrial fibroblasts and myofibroblasts
Relative quantities *versus* GAPDH of Na_v α (*A*) and β (*B*) subunit transcripts evaluated by real-time reverse transcription polymerase chain reaction (RT-qPCR) using mRNA extract from human atrial fibroblasts after 3–7 (fibroblasts) or 13–17 (myofibroblasts) days of culture.

Discussion

This study investigates for the first time changes in the expression pattern of VGSCs associated with human atrial fibroblasts differentiation. We show that human atrial fibroblasts differentiation into myofibroblasts is accompanied by the neo-expression of rapid voltage gated sodium current. Electrophysiological properties of this current are similar to sodium channels found in cardiac myocytes and there is strong evidence that this current is supported by $Na_v1.5$ α-subunit, the typical cardiac VGSC traditionally characterized in cardiomyocytes.

Fibroblasts differentiation was studied in culture as described in previous studies (Baudino *et al.* 2006; Teunissen *et al.* 2007; Benamer *et al.* 2009; Benamer *et al.* 2011). In our experimental conditions, the cells expressed α-SMA, a typical marker of myofibroblasts (Wang *et al.* 2003; Miragoli *et al.* 2006; Miragoli *et al.* 2007; Zlochiver *et al.* 2008), between 7 and 12 days of culture. This suggests that human atrial fibroblasts in culture differentiate into myofibroblasts within this period of time. The differentiation process is slower than that described previously in our laboratory using mouse ventricular fibroblasts (Benamer *et al.* 2009; Benamer *et al.* 2011). Since the present study was realized in the same conditions, we suggest that the differentiation kinetics depend on either the species and/or on the origin of the fibroblast (atrial or ventricular).

Investigating the VGSC α-subunit candidates revealed that $Na_v1.2$, $Na_v1.3$, $Na_v1.5$, $Na_v1.6$ and $Na_v1.7$ transcripts are present. The use of the real time RT-qPCR technique on diverse cell differentiation states allowed us to compare the expression levels of all sodium channel isoforms found in human genome within fibroblasts or myofibroblasts. The differentiation process is accompanied by an increased expression of the cardiac $Na_v1.5$ transcripts and by a slight *de novo* expression of neuronal transcripts such as $Na_v1.3$, $Na_v1.6$ and $Na_v1.7$. However, neuronal VGSCs are weakly expressed compared to $Na_v1.5$. According to our results, there is no transcript of $Na_v1.3$, $Na_v1.6$ and $Na_v1.7$ in fibroblasts whereas they were detected in a previous study of Li *et al.* (2009*a*). At least two hypotheses may account for this discrepancy. First, Li's study used a commercially available fibroblast cell line culture with several passages. As a consequence, it is reasonable to postulate that the cells they handled were (at least in major part) myofibroblasts, rather than fibroblasts. The detection of $Na_v1.3$, $Na_v1.6$ and $Na_v1.7$ would thus correspond to myofibroblast transcripts as in our study. Moreover, there may be differences between the expression pattern of ventricular (as in Li's study) and atrial (as in ours) fibroblasts. Amongst detected transcripts in

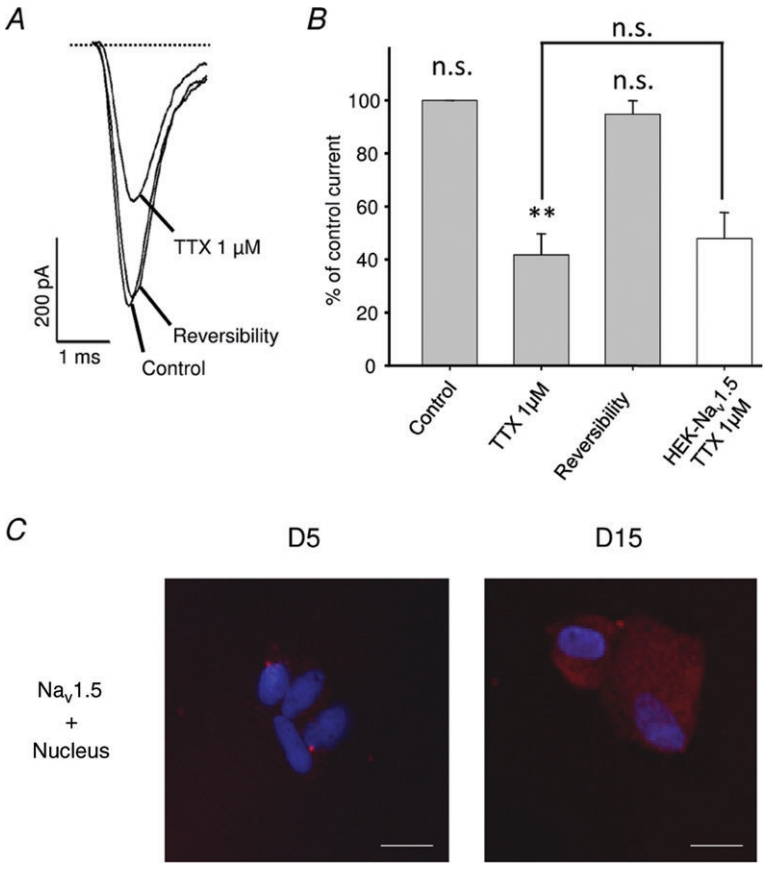

Figure 5. Molecular identity of the VGSC α-subunit recorded in human atrial myofibroblasts
A, representative example of the effect of TTX at 1 μM on fibroblast sodium current. Currents were elicited by a standard test pulse from a holding potential of −120 mV to a test pulse of −20 mV for 50 ms. TTX was perfused until current stabilization and washout with a control perfusion to check reversibility. *B*, effects of 1 μM TTX ($n = 4$) on the voltage gated sodium current evoked as described in *A* on myofibroblasts (grey bars) or HEK293 cells transiently transfected with $Na_v1.5 + \beta_1$ subunits (white bar). *C*, fibroblasts (5 days of culture; D5) and myofibroblasts (15 days of culture; D15) observed in fluorescence. Cells were stained with anti-$Na_v1.5$ antibody and the nuclei were stained using TO-PRO-3. Scale bar corresponds to 20 μm.

myofibroblasts, $Na_v1.5$ is the only one translated in a TTX resistant subunit (Catterall *et al.* 2005). In this study, 1 μM blocked almost 50% of the current as observed in $Na_v1.5$ transfected HEK293T cells. This result strongly suggests that $Na_v1.5$ is the α-subunit responsible of the current. Whereas real time RT-qPCR and TTX results, combined with immunofluorescence experiments, do not rule out the presence of TTX sensitive isoforms, they clearly indicate that the $Na_v1.5$ α-subunit represents the major part of the human myofibroblast's VGSC. Moreover, based on the TTX sensitivity and kinetics of the current we can also exclude a calcium channels component.

In the present study, it would have been interesting to compare sodium current from myofibroblasts and atrial myocytes of the same patients. Unfortunately, whereas cardiomyocytes and fibroblasts can be obtained using the same protocol, it is difficult to obtain both cell types at the same time since enzymatic digestion has to be adapted to the cells desired. Comparing the VGSC current of the present study to those observed in mammalian cardiomyocytes revealed similar but not identical biophysical properties (Schneider *et al.* 1994; Li *et al.* 2009*b*; Sato *et al.* 2009; Mishra *et al.* 2011; Lin *et al.* 2011). For example, the window current delimited by the area between the activation and inactivation is larger in myofibroblasts. This defines a range of potentials where the sodium channels can be activated without being fully inactivated, leading to a persistent entry of sodium ions in myofibroblasts. How relevant can a steady-state availability of 0.37% at -60 mV be? A recent study showed that $Na_v1.5$ Y1767C mutant which presents a value of 0.13% is implicated in long QT syndrome development (Huang *et al.* 2010). It is therefore reasonable to envisage that the persistent entry of sodium in myofibroblasts through the window current may have a significant impact on their function.

According to the window current characterized in our study, the persistent sodium entry strongly depends on membrane potential. Despite that fibroblast and myofibroblasts are not considered to be excitable, different studies have shown membrane potential variations of these cells. In human and rat atrial fibroblasts, the resting membrane potential is close to -15 mV (Kiseleva *et al.* 1998; Kamkin *et al.* 1999). At this potential, the persistent entry of sodium predicted with the Boltzmann product would be negligible (see Fig. 3*B*). On the other hand, several phenomena lead to a negative shift of fibroblast membrane potential recorded in atrial tissue. Indeed, experiments realized on rat atrial fibroblasts revealed a stretch-dependent strong hyperpolarization of membrane potential that was maximal 8 days after myocardial infarction and recovered after 30 days (Kiseleva *et al.* 1998; Kamkin *et al.* 2002). Another study realized in the same cardiac tissue showed that reoxygenation after hypoxia also induced a hyperpolarization of rat atrial fibroblast membrane potential (Kamkin *et al.* 2003*b*). Whereas it is difficult to test the effect of these post-traumatic conditions on membrane potential in human atrial tissue, it is reasonable to envisage that similar mechanisms could take place. In rat, these potentials, predominantly between -50 mV and -60 mV, correspond to the peak of the sodium window current described in the present study. As a consequence, such a cell polarity may induce a persistent sodium entry. In rat myofibroblasts, the sodium–calcium exchanger has been shown to be implicated in migration and proliferation processes (Raizman *et al.* 2007). It is therefore plausible that the persistent sodium current could lead to similar effects through an increase in intracellular calcium due to the reverse mode of the sodium–calcium exchanger. It would be interesting to investigate whether $Na_v1.5$ could influence myofibroblast proliferation, migration and secretion properties as observed in other cell types (Roger *et al.* 2003; Zhao *et al.* 2008; Gillet *et al.* 2009; Andrikopoulos *et al.* 2011). Moreover, an increase in calcium has recently been related to fibrogenesis in human atrial fibrillation (Du *et al.* 2010). In this study, intracellular calcium modulation was mediated by TRPM7 expression in human atrial fibroblasts and was modulated with fibroblast differentiation. Our study raises the possibility that $Na_v1.5$, through the reverse mode of the sodium–calcium exchanger, participates in such an increase in intracellular calcium in myofibroblasts and could be implicated in human atrial fibrosis and fibrillation.

In summary, we show for the first time the presence of a rapid voltage gated sodium current in human atrial myofibroblasts with electrophysiological characteristics similar to sodium channels found in excitable cells. Multiple arguments support that this sodium current is predominantly supported by the $Na_v1.5$ α subunit, which may generate a persistent sodium entry into myofibroblasts. Since fibrosis is one of the fundamental mechanisms implicated in atrial fibrillation, it is of great interest to investigate how this current could influence myofibroblasts proliferation, migration and secretion properties. Moreover, several $Na_v1.5$ mutations are related to cardiac pathologies (Amin *et al.* 2010) such as Long QT, Brugada syndrome or Lenegre disease. This study raises the possibility that some cardiac consequences of such mutations may be due to myofibroblast alterations. For example, a SCN5A mutation associated with lone atrial fibrillation has recently been characterized as a gain of function mutation that enhances the sodium window current (Li *et al.* 2009*c*). Since atrial fibrosis is strongly related to atrial fibrillation, it would be interesting to question the impact of this mutation on atrial myofibroblast physiology.

In conclusion, this study provides a new direction in research on the cardiac role of wild-type $Na_v1.5$ as well as the consequences of $Na_v1.5$ pathological mutations.

Therefore, investigating the expression and role of $Na_v1.5$ sodium channels of myofibroblasts in the atria during the remodelling in pathologies such as atrial fibrillation is warranted.

References

Allessie M, Ausma J & Schotten U (2002). Electrical, contractile and structural remodeling during atrial fibrillation. *Cardiovasc Res* **54**, 230–246.

Amin AS, Tan HL & Wilde AA (2010). Cardiac ion channels in health and disease. *Heart Rhythm* **7**, 117–126.

Ancey C, Corbi P, Froger J, Delwail A, Wijdenes J, Gascan H, Potreau D & Lecron JC (2002). Secretion of IL-6, IL-11 and LIF by human cardiomyocytes in primary culture. *Cytokine* **18**, 199–205.

Andrikopoulos P, Fraser SP, Patterson L, Ahmad Z, Burcu H, Ottaviani D, Diss JK, Box C, Eccles SA & Djamgoz MB (2011). Angiogenic functions of voltage-gated Na^+ channels in human endothelial cells: modulation of vascular endothelial growth factor (VEGF) signaling. *J Biol Chem* **286**, 16846–16860.

Armstrong CM & Hille B (1998). Voltage-gated ion channels and electrical excitability. *Neuron* **20**, 371–380.

Baudino TA, Carver W, Giles W & Borg TK (2006). Cardiac fibroblasts: friend or foe? *Am J Physiol Heart Circ Physiol* **291**, H1015–H1026.

Benamer N, Fares N, Bois P & Faivre JF (2011). Electrophysiological and functional effects of sphingosine-1-phosphate in mouse ventricular fibroblasts. *Biochem Biophys Res Commun* **408**, 6–11.

Benamer N, Moha Ou MH, Demolombe S, Cantereau A, Delwail A, Bois P, Bescond J & Faivre JF (2009). Molecular and functional characterization of a new potassium conductance in mouse ventricular fibroblasts. *J Mol Cell Cardiol* **46**, 508–517.

Black JA, Liu S & Waxman SG (2009). Sodium channel activity modulates multiple functions in microglia. *Glia* **57**, 1072–1081.

Brilla CG, Maisch B, Zhou G & Weber KT (1995). Hormonal regulation of cardiac fibroblast function. *Eur Heart J* **16 Suppl C**, 45–50.

Burstein B, Libby E, Calderone A & Nattel S (2008). Differential behaviors of atrial versus ventricular fibroblasts: a potential role for platelet-derived growth factor in atrial-ventricular remodeling differences. *Circulation* **117**, 1630–1641.

Burstein B & Nattel S (2008). Atrial fibrosis: mechanisms and clinical relevance in atrial fibrillation. *J Am Coll Cardiol* **51**, 802–809.

Catterall WA (1986). Molecular properties of voltage-sensitive sodium channels. *Annu Rev Biochem* **55**, 953–985.

Catterall WA, Goldin AL & Waxman SG (2005). International Union of Pharmacology. XLVII. Nomenclature and structure-function relationships of voltage-gated sodium channels. *Pharmacol Rev* **57**, 397–409.

Chilton L, Ohya S, Freed D, George E, Drobic V, Shibukawa Y, Maccannell KA, Imaizumi Y, Clark RB, Dixon IM & Giles WR (2005). K^+ currents regulate the resting membrane potential, proliferation, and contractile responses in ventricular fibroblasts and myofibroblasts. *Am J Physiol Heart Circ Physiol* **288**, H2931–H2939.

Du J, Xie J, Zhang Z, Tsujikawa H, Fusco D, Silverman D, Liang B & Yue L (2010). TRPM7-mediated Ca^{2+} signals confer fibrogenesis in human atrial fibrillation. *Circ Res* **106**, 992–1003.

El Chemaly A, Guinamard R, Demion M, Fares N, Jebara V, Faivre JF & Bois P (2006). A voltage-activated proton current in human cardiac fibroblasts. *Biochem Biophys Res Commun* **340**, 512–516.

Ellmers LJ, Knowles JW, Kim HS, Smithies O, Maeda N & Cameron VA (2002). Ventricular expression of natriuretic peptides in Npr1(–/–) mice with cardiac hypertrophy and fibrosis. *Am J Physiol Heart Circ Physiol* **283**, H707–H714.

Fozzard HA & Hanck DA (1996). Structure and function of voltage-dependent sodium channels: comparison of brain II and cardiac isoforms. *Physiol Rev* **76**, 887–926.

Gillet L, Roger S, Besson P, Lecaille F, Gore J, Bougnoux P, Lalmanach G & Le Guennec JY (2009). Voltage-gated sodium channel activity promotes cysteine cathepsin-dependent invasiveness and colony growth of human cancer cells. *J Biol Chem* **284**, 8680–8691.

Hatem SN, Benardeau A, Rucker-Martin C, Marty I, de CP, Villaz M & Mercadier JJ (1997). Different compartments of sarcoplasmic reticulum participate in the excitation-contraction coupling process in human atrial myocytes. *Circ Res* **80**, 345–353.

Huang H, Priori SG, Napolitano C, O'Leary ME & Chahine M (2010). Y1767C, a novel SCN5A mutation induces a persistent sodium current and potentiates ranolazine inhibition of Nav1.5 channels. *Am J Physiol Heart Circ Physiol* **300**, H288–299.

Kamkin A, Kiseleva I & Isenberg G (2003*a*). Activation and inactivation of a non-selective cation conductance by local mechanical deformation of acutely isolated cardiac fibroblasts. *Cardiovasc Res* **57**, 793–803.

Kamkin A, Kiseleva I, Wagner KD, Lammerich A, Bohm J, Persson PB & Gunther J (1999). Mechanically induced potentials in fibroblasts from human right atrium. *Exp Physiol* **84**, 347–356.

Kamkin A, Kiseleva I, Wagner KD, Lozinsky I, Gunther J & Scholz H (2003*b*). Mechanically induced potentials in atrial fibroblasts from rat hearts are sensitive to hypoxia/reoxygenation. *Pflugers Arch* **446**, 169–174.

Kamkin A, Kiseleva I, Wagner KD, Pylaev A, Leiterer KP, Theres H, Scholz H, Gunther J & Isenberg G (2002). A possible role for atrial fibroblasts in postinfarction bradycardia. *Am J Physiol Heart Circ Physiol* **282**, H842–H849.

Kiseleva I, Kamkin A, Pylaev A, Kondratjev D, Leiterer KP, Theres H, Wagner KD, Persson PB & Gunther J (1998). Electrophysiological properties of mechanosensitive atrial fibroblasts from chronic infarcted rat heart. *J Mol Cell Cardiol* **30**, 1083–1093.

Li GR, Sun HY, Chen JB, Zhou Y, Tse HF & Lau CP (2009*a*). Characterization of multiple ion channels in cultured human cardiac fibroblasts. *PLoS One* **4**, e7307.

Li GR, Sun HY, Zhang XH, Cheng LC, Chiu SW, Tse HF & Lau CP (2009*b*). Omega-3 polyunsaturated fatty acids inhibit transient outward and ultra-rapid delayed rectifier K^+ currents and Na^+ current in human atrial myocytes. *Cardiovasc Res* **81**, 286–293.

Li Q, Huang H, Liu G, Lam K, Rutberg J, Green MS, Birnie DH, Lemery R, Chahine M & Gollob MH (2009*c*). Gain-of-function mutation of Nav1.5 in atrial fibrillation enhances cellular excitability and lowers the threshold for action potential firing. *Biochem Biophys Res Commun* **380**, 132–137.

Lin X, Liu N, Lu J, Zhang J, Anumonwo JM, Isom LL, Fishman GI & Delmar M (2011). Subcellular heterogeneity of sodium current properties in adult cardiac ventricular myocytes. *Heart Rhythm* **8**, 1923–1930.

Louault C, Benamer N, Faivre JF, Potreau D & Bescond J (2008). Implication of connexins 40 and 43 in functional coupling between mouse cardiac fibroblasts in primary culture. *Biochim Biophys Acta* **1778**, 2097–2104.

Manabe I, Shindo T & Nagai R (2002). Gene expression in fibroblasts and fibrosis: involvement in cardiac hypertrophy. *Circ Res* **91**, 1103–1113.

Margolskee RF, McHendry-Rinde B & Horn R (1993). Panning transfected cells for electrophysiological studies. *Biotechniques* **15**, 906–911.

Miragoli M, Gaudesius G & Rohr S (2006). Electrotonic modulation of cardiac impulse conduction by myofibroblasts. *Circ Res* **98**, 801–810.

Miragoli M, Salvarani N & Rohr S (2007). Myofibroblasts induce ectopic activity in cardiac tissue. *Circ Res* **101**, 755–758.

Mishra S, Undrovinas NA, Maltsev VA, Reznikov V, Sabbah HN & Undrovinas A (2011). Post-transcriptional silencing of SCN1B and SCN2B genes modulates late sodium current in cardiac myocytes from normal dogs and dogs with chronic heart failure. *Am J Physiol Heart Circ Physiol* **301**, H1596–1605.

Nakajima H, Nakajima HO, Salcher O, Dittie AS, Dembowsky K, Jing S & Field LJ (2000). Atrial but not ventricular fibrosis in mice expressing a mutant transforming growth factor-β_1 transgene in the heart. *Circ Res* **86**, 571–579.

Raizman JE, Komljenovic J, Chang R, Deng C, Bedosky KM, Rattan SG, Cunnington RH, Freed DH & Dixon IM (2007). The participation of the Na^+-Ca^{2+} exchanger in primary cardiac myofibroblast migration, contraction, and proliferation. *J Cell Physiol* **213**, 540–551.

Roger S, Besson P & Le Guennec JY (2003). Involvement of a novel fast inward sodium current in the invasion capacity of a breast cancer cell line. *Biochim Biophys Acta* **1616**, 107–111.

Rose RA, Hatano N, Ohya S, Imaizumi Y & Giles WR (2007). C-type natriuretic peptide activates a non-selective cation current in acutely isolated rat cardiac fibroblasts via natriuretic peptide C receptor-mediated signalling. *J Physiol* **580**, 255–274.

Sato PY, Musa H, Coombs W, Guerrero-Serna G, Patino GA, Taffet SM, Isom LL & Delmar M (2009). Loss of plakophilin-2 expression leads to decreased sodium current and slower conduction velocity in cultured cardiac myocytes. *Circ Res* **105**, 523–526.

Schneider M, Proebstle T, Hombach V, Hannekum A & Rudel R (1994). Characterization of the sodium currents in isolated human cardiocytes. *Pflugers Arch* **428**, 84–90.

Schotten U, Verheule S, Kirchhof P & Goette A (2011). Pathophysiological mechanisms of atrial fibrillation: a translational appraisal. *Physiol Rev* **91**, 265–325.

Shibukawa Y, Chilton EL, Maccannell KA, Clark RB & Giles WR (2005). K^+ currents activated by depolarization in cardiac fibroblasts. *Biophys J* **88**, 3924–3935.

Swynghedauw B (1999). Molecular mechanisms of myocardial remodeling. *Physiol Rev* **79**, 215–262.

Teunissen BE, Smeets PJ, Willemsen PH, De Windt LJ, Van der Vusse GL & Van Bilsen M (2007). Activation of PPARdelta inhibits cardiac fibroblast proliferation and the transdifferentiation into myofibroblasts. *Cardiovasc Res* **75**, 519–529.

Vasquez C, Benamer N & Morley GE (2011). The cardiac fibroblast: functional and electrophysiological considerations in healthy and diseased hearts. *J Cardiovasc Pharmacol* **57**, 380–388.

Verheule S, Sato T, Everett T 4th, Engle SK, Otten D, Rubart-von der Lohe M, Nakajima HO, Nakajima H, Field LJ & Olgin JE (2004). Increased vulnerability to atrial fibrillation in transgenic mice with selective atrial fibrosis caused by overexpression of TGF-β1. *Circ Res* **94**, 1458–1465.

Wang J, Chen H, Seth A & McCulloch CA (2003). Mechanical force regulation of myofibroblast differentiation in cardiac fibroblasts. *Am J Physiol Heart Circ Physiol* **285**, H1871–H1881.

Weber KT, Sun Y, Tyagi SC & Cleutjens JP (1994). Collagen network of the myocardium: function, structural remodeling and regulatory mechanisms. *J Mol Cell Cardiol* **26**, 279–292.

Xiao HD, Fuchs S, Campbell DJ, Lewis W, Dudley SC Jr, Kasi VS, Hoit BD, Keshelava G, Zhao H, Capecchi MR & Bernstein KE (2004). Mice with cardiac-restricted angiotensin-converting enzyme (ACE) have atrial enlargement, cardiac arrhythmia, and sudden death. *Am J Pathol* **165**, 1019–1032.

Yue L, Xie J & Nattel S (2011). Molecular determinants of cardiac fibroblast electrical function and therapeutic implications for atrial fibrillation. *Cardiovasc Res* **89**, 744–753.

Zhao P, Barr TP, Hou Q, Dib-Hajj SD, Black JA, Albrecht PJ, Petersen K, Eisenberg E, Wymer JP, Rice FL & Waxman SG (2008). Voltage-gated sodium channel expression in rat and human epidermal keratinocytes: evidence for a role in pain. *Pain* **139**, 90–105.

Zlochiver S, Munoz V, Vikstrom KL, Taffet SM, Berenfeld O & Jalife J (2008). Electrotonic myofibroblast-to-myocyte coupling increases propensity to reentrant arrhythmias in two-dimensional cardiac monolayers. *Biophys J* **95**, 4469–4480.

Author contributions

A.C., P.C., P.B., M.C. and J.F.F. contributed to the conception and design of the experiments. A.C., A.M., B.T., O.T., M.M. and N.B. performed data collection, analysis and/or interpretation. A.C.,

P.B., M.C. and J.F.F. drafted or critically revised the manuscript. qPCR experiments were done at the Institut Universitaire en Sant Mentale de Qubec (Qubec, Canada). All other experiments were performed at the Institut de Physiologie et Biologie Cellulaire (Poitiers, France). All authors approved the final version submitted.

Acknowledgements

The authors are grateful to Christophe Magaud for his expert technical assistance and to ImageUp microscopic platform for fluorescence imaging. This work was supported in part by the Fondation de France. The authors declare no conflict of interest in relation to this article.

Translational perspective

Fibroblasts play a major role in heart physiology. They are at the origin of the extracellular matrix renewal and production of various paracrine and autocrine factors. In pathological conditions, fibroblasts proliferate, migrate and differentiate into myofibroblasts leading to cardiac fibrosis. This differentiated status is associated with changes in gene expression profile, leading to neo-expression of proteins such as ionic channels. We demonstrate that the activity of voltage-gated sodium channels increases as human atrial fibroblasts differentiate into myofibroblasts. It can be hypothesized that during the fibrosis process characterized by fibroblast differentiation the sodium channel modulation in these non-excitable cells may contribute to a pathological phenotype. Since fibrosis is one of the fundamental mechanisms involved in atrial fibrillation, it may be of great interest to investigate how this current could influence myofibroblast proliferation, migration and secretion properties. On the other hand, several sodium channel mutations are related to cardiac pathologies such as long QT, Brugada syndrome and Lenegre disease. This study raises the possibility that some cardiac consequences of such mutations may be due to myofibroblasts in addition to cardiac muscular cell alteration. In conclusion, this study provides a new direction in research on the cardiac role of sodium channels.